Minireview

# *Wolinella succinogenes* quinol:fumarate reductase and its comparison to *E. coli* succinate:quinone reductase

C. Roy D. Lancaster*

*Max-Planck-Institut für Biophysik, Abteilung Molekulare Membranbiologie, Marie-Curie-Str. 15, D-60439 Frankfurt am Main, Germany*

Received 25 August 2003; accepted 1 September 2003

First published online 9 October 2003

Edited by Gunnar von Heijne, Jan Rydström and Peter Brzezinski

**Abstract The three-dimensional structure of *Wolinella succinogenes* quinol:fumarate reductase (QFR), a dihaem-containing member of the superfamily of succinate:quinone oxidoreductases (SQOR), has been determined at 2.2 Å resolution by X-ray crystallography [Lancaster et al., Nature 402 (1999) 377–385]. The structure and mechanism of *W. succinogenes* QFR and their relevance to the SQOR superfamily have recently been reviewed [Lancaster, Adv. Protein Chem. 63 (2003) 131–149]. Here, a comparison is presented of *W. succinogenes* QFR to the recently determined structure of the monohaem containing succinate:quinone reductase from *Escherichia coli* [Yankovskaya et al., Science 299 (2003) 700–704]. In spite of differences in polypeptide and haem composition, the overall topology of the membrane anchors and their relative orientation to the conserved hydrophilic subunits is strikingly similar. A major difference is the lack of any evidence for a 'proximal' quinone site, close to the hydrophilic subunits, in *W. succinogenes* QFR.**



*Key words:* Atomic model; Bioenergetics; Fumarate reductase; Membrane protein; Succinate dehydrogenase; X-ray crystallography

## 1. Introduction

Succinate:quinone oxidoreductases (SQORs; EC 1.3.5.1 [1]) are enzymes that couple the two-electron oxidation of succinate to fumarate (reaction 1) to the two-electron reduction of quinone to quinol (reaction 2).

$$\text{succinate} \rightleftarrows \text{fumarate} + 2H^+ + 2e^- \quad (1)$$

$$\text{quinone} + 2H^+ + 2e^- \rightleftarrows \text{quinol} \quad (2)$$

They can also catalyse the opposite reaction, the coupling of quinol oxidation to the reduction of fumarate [2]. Depending on the direction of the reaction catalysed in vivo, the members of the superfamily of SQORs can be classified as either succinate:quinone reductases (SQR) or quinol:fumarate reductases (QFR) [3]. SQR and QFR complexes are anchored in the cytoplasmic membranes of archaebacteria, eubacteria and in the inner mitochondrial membrane of eukaryotes with the hydrophilic domain extending into the cytoplasm and the mitochondrial matrix, respectively. SQR (respiratory complex II) is involved in aerobic metabolism as part of the citric acid cycle (Krebs cycle) and of the aerobic respiratory chain [4]. QFR participates in anaerobic respiration with fumarate as the terminal electron acceptor [5–7], and is part of the electron transport chain catalysing the oxidation of various donor substrates (e.g. $H_2$ or formate) by fumarate. These reactions are coupled via an electrochemical proton potential ($\Delta p$) [8] to ADP phosphorylation with inorganic phosphate by ATP synthase.

## 2. SQOR classification

SQORs generally contain four protein subunits, referred to as A, B, C and D. Subunits A and B are hydrophilic, whereas subunits C and D are integral membrane proteins. Among species, subunits A and B have high sequence homology, while that for the hydrophobic subunits is much lower. Most of the SQR enzymes of Gram-positive bacteria and the QFR enzymes from ε-proteobacteria contain only one larger hydrophobic polypeptide (C), which is thought to have evolved from a fusion of the genes for the two smaller subunits C and D [9–11]. While subunit A harbours the site of fumarate reduction and succinate oxidation, the hydrophobic subunit(s) contain the site of quinol oxidation and quinone reduction.

Based on their hydrophobic domain and haem *b* content [9,10], SQORs can be classified in five types (Fig. 1a). Type A enzymes contain two hydrophobic subunits and two haem groups, e.g. SQR from the archaea *Archaeoglobus fulgidus*, *Natronomonas pharaonis* and *Thermoplasma acidophilum*. Type B enzymes contain one hydrophobic subunit and two haem groups, as is the case for SQR from the Gram-positive bacteria *Bacillus subtilis*, *Paenibacillus macerans* and QFR from the ε-proteobacteria *Campylobacter jejuni*, *Helicobacter pylori*, and *Wolinella succinogenes*. Examples for type C enzymes, which possess two hydrophobic subunits and one haem group, are SQR from mammalian mitochondria and from the proteobacteria *Paracoccus denitrificans* and *Escherichia coli* and QFR from the nematode *Ascaris suum*. The QFR of *E. coli* is an example of a type D enzyme, which contains two hydrophobic subunits and no haem group. Finally, type E enzymes, such as SQRs from the archaea *Aci-*

*http://www.mpibp-frankfurt.mpg.de/lancaster/complexII/index.html.
*E-mail address:* roy.lancaster@mpibp-frankfurt.mpg.de (C.R.D. Lancaster).

0014-5793/03/$22.00 
doi:10.1016/S0014-5793(03)01100-1

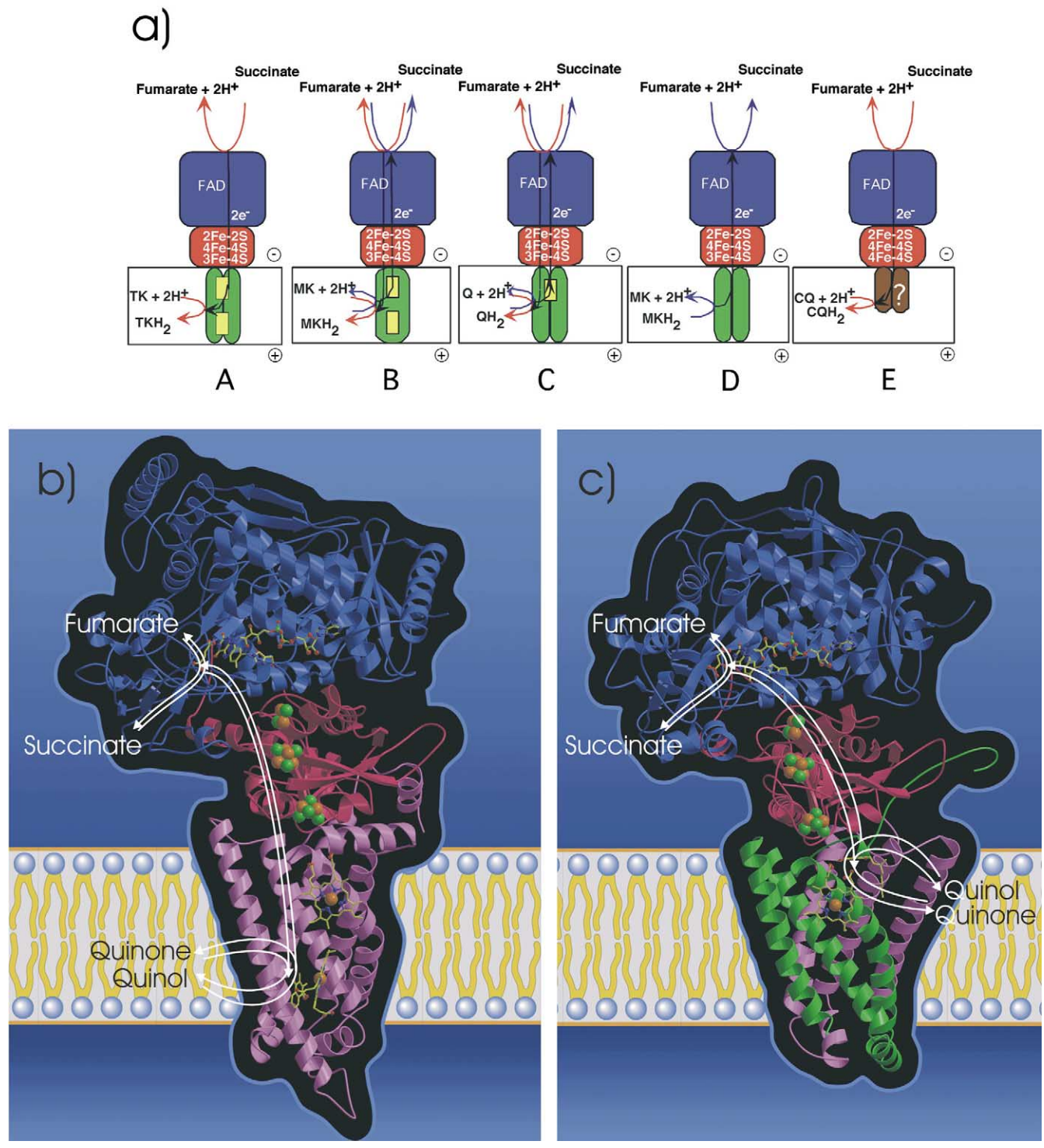


Fig. 1. a: Classification (A–E) of SQORs based on their hydrophobic domain and haem content. The hydrophilic subunits A and B are drawn schematically in blue and red, respectively, the hydrophobic subunits C and D in green. Haem groups are symbolised by small rectangles. The directions of the reactions catalysed by SQR and QFR are indicated by red and blue arrows, respectively. White rectangles symbolise the respective cytoplasmic or inner mitochondrial membrane bilayer. The positive (+) and negative (−) sides of the membrane are indicated. In bacteria, the negative side is the cytoplasm ('inside'), the positive side the periplasm ('outside'). For mitochondrial systems, these are the mitochondrial matrix and the intermembrane space, respectively. The type of quinone transformed in vivo is not necessarily unique for each type of enzyme. The examples given are thermoplasma-quinone (TK), menaquinone (MK), ubiquinone (Q), and caldariella quinone (CQ) [3,46]. b,c: Three-dimensional structures of *W. succinogenes* QFR, a B-type SQOR (b [11]) and *E. coli* SQR, a C-type SQOR (c [14]) The Cα traces of the A subunits are shown in blue, those of the B subunits in red, those of the C subunits in pink, and those of the D subunits in green. The atomic structures of the prosthetic groups are superimposed for better visibility. From top to bottom, these are the covalently bound FAD, the [2Fe–2S], the [4Fe–4S], and the [3Fe–4S] iron–sulphur clusters, the proximal (and, where present) the distal haem *b* groups. Atomic colour coding is as follows: C, N, O, P, S and Fe are displayed in yellow, blue, red, light green, green, and orange, respectively. Figures with atomic models were prepared with a version of Molscript [47] modified for colour ramping [48] and rendered with the program Raster3D [49].

*dianus ambivalens* and *Sulfolobus acidocaldarius*, but also from the proteobacterium *C. jejuni* and the cyanobacterium *Synechocystis*, also contain no haem, but have two hydrophobic subunits very different from the other four types and more similar to those of heterodisulphide reductase from methanogenic archaea [12].

## 3. SQOR structure and function

### 3.1. Overall description of the structure

The currently available crystal structures of SQORs are those of two prokaryotic QFRs, both since 1999, and one prokaryotic SQR, since 2003. The *E. coli* QFR, determined at 3.3 Å resolution [13], belongs to the type D enzymes, and the QFR of *W. succinogenes* (Fig. 1b), refined at 2.2 Å resolution [11], is of type B. The structure of the SQR from *E. coli* (Fig. 1c) was reported at 2.6 Å resolution [14]. Interestingly, *E. coli* QFR appears to be a monomeric complex of one copy each of the A, B, C and D subunits, whereas *W. succinogenes* QFR is apparently a homodimer of two sets of A, B and C subunits, and *E. coli* SQR is a homotrimer of three sets of A, B, C and D subunits. At least for the *Wolinella* enzyme, it has been derived from analytical gel filtration experiments that the homodimer is apparently also present in the detergent-solubilised state of the enzyme [15], implying that it is unlikely to be an artifact of crystallisation. However, functionally both *W. succinogenes* QFR and *E. coli* SQR appear to act as monomers, which is why only the monomeric complexes are shown in Fig. 1b,c.

The structures of *E. coli* QFR and *W. succinogenes* QFR have been compared earlier [11,15], as have the structures of *E. coli* QFR and SQR [16]. Therefore, this contribution will focus mainly on the comparison of *W. succinogenes* QFR and *E. coli* SQR.

### 3.2. The relative orientations of soluble and membrane-embedded SQOR subunits

The structures of all three SQOR enzymes of known structure can be superimposed on the basis of the Cα positions of the conserved hydrophilic subunits A and B. In spite of differences in polypeptide and haem composition, the overall topology of the membrane anchors and their relative orientation to the conserved hydrophilic subunits is strikingly similar in the case of *W. succinogenes* QFR and *E. coli* SQR (Fig. 2), but not for *E. coli* QFR. However, as demonstrated earlier (cf. figs. 3d and 6c in [11]), in an alternate orientation the transmembrane subunits of *E. coli* QFR and of *W. succinogenes* QFR can be overlaid in spite of the respective absence and presence of the two haem groups. Consequently, the relative orientations of the hydrophilic subunits and the transmembrane subunits are similar in *W. succinogenes* QFR and *E. coli* SQR and different in *E. coli* QFR.

### 3.3. Subunit A, and the site of succinate oxidation/fumarate reduction

The flavoprotein or A subunit (64–73 kDa) of all described membrane-bound SQOR complexes contains a flavin adenine dinucleotide (FAD) prosthetic group covalently bound to a conserved His residue as an 8α-[*N*ε-histidyl]-FAD] [17–20]. The two most important domains of subunit A are the bipartite FAD-binding domain and the 'capping' domain, which is inserted between the two parts of the FAD-binding domain. The capping domain contributes to burying the otherwise solvent-exposed FAD isoalloxazine ring from the protein surface.

The binding site of succinate/fumarate is located between the FAD-binding domain and the capping domain next to the plane of the FAD isoalloxazine ring [11]. The structures and results from site-directed mutagenesis [21] suggest that the

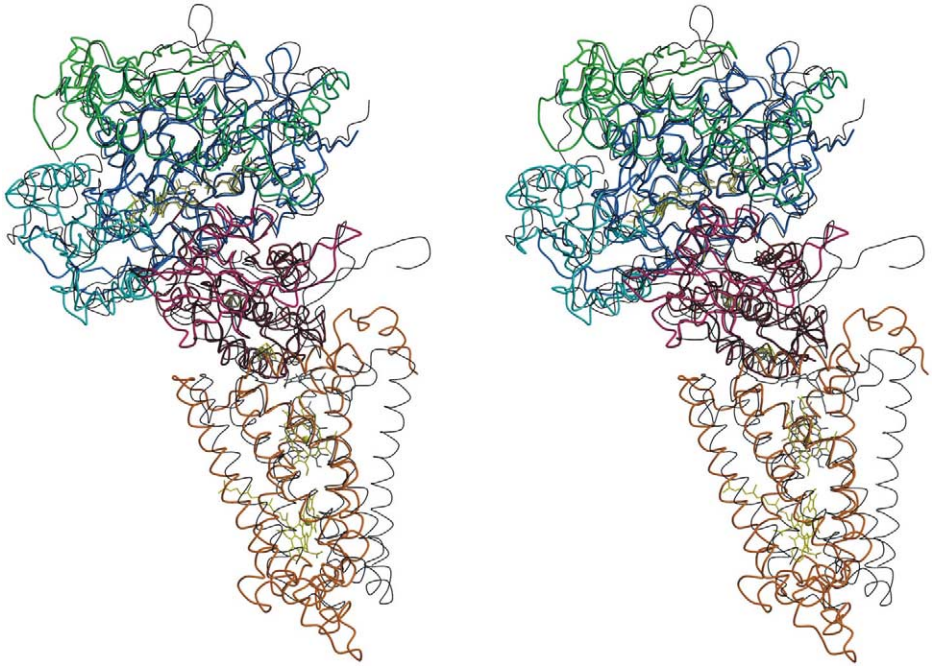

Fig. 2. Comparison of the structures of *W. succinogenes* QFR (in colour, with cofactors in yellow) and *E. coli* SQR (in black, with cofactors in grey). Subunit A of *W. succinogenes* QFR is drawn in blue (FAD-binding domain), light blue (capping domain), green (helical domain), and light green (C-terminal domain), subunit B is shown in pink (N-terminal domain) and brown (C-terminal domain), and subunit C in orange. The positions of 782 Cα atoms could be superimposed with an rms deviation of 1.7 Å.

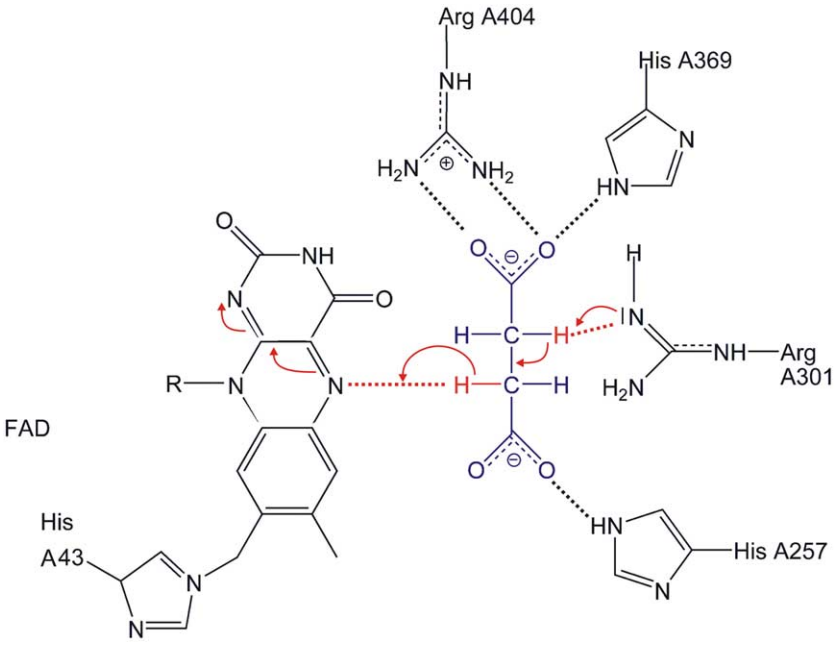


Fig. 3. Possible mechanism of succinate oxidation/fumarate reduction. Figure modified from [21].

*trans*-dehydrogenation of succinate to fumarate occurs by the combination of a hydride ion transfer from one succinate methylene group to the N5 position of the FAD and of a proton transfer from the other succinate methylene group to the side chain of a conserved Arg residue of the capping domain (Fig. 3). All residues implicated in substrate binding and catalysis are conserved throughout the superfamily of SQORs, so that this reversible mechanism is considered generally relevant for all SQORs. Release of the product could be facilitated by movement of the capping domain away from the dicarboxylate site [11,21].

### 3.4. Subunit B, the iron–sulphur protein

Generally, SQORs contain three iron–sulphur clusters, which are exclusively bound by the B subunit of 26–30 kDa. Enzyme types A–D contain one $[2Fe–2S]^{2+,1+}$, one $[4Fe–4S]^{2+,1+}$ and one $[3Fe–4S]^{1+,0}$ cluster, whereas an additional $[4Fe–4S]^{2+,1+}$ cluster apparently replaces the $[3Fe–4S]^{1+,0}$ in the type E enzyme [22]. This subunit consists of two domains, an N-terminal 'plant ferredoxin' domain, in contact with subunit A and binding the [2Fe–2S] iron–sulphur cluster, and a C-terminal 'bacterial ferredoxin' domain, in contact with the hydrophobic subunit(s) and binding the [4Fe–4S] and the [3Fe–4S] iron–sulphur clusters. In general, these iron–sulphur clusters are co-ordinated by conserved Cys residues, although one of the ligands to the [2Fe–2S] cluster in *E. coli* SQR is an Asp. At the position corresponding to the fourth Cys of the [4Fe–4S] cluster, the [3Fe–4S] cluster contains a Leu (*W. succinogenes* QFR), Ile (*E. coli* SQR), Val (*E. coli* QFR), or Ser (*B. subtilis* SQR). Whereas the introduction of a Cys into *E. coli* QFR [23] could replace the native [3Fe–4S] by a [4Fe–4S] cluster, this was not the case for *B. subtilis* SQR [24].

### 3.5. The integral membrane subunit(s) C (and D) and the sites of quinol oxidation/quinone reduction

Type A, C and D SQOR enzymes contain two hydrophobic polypeptides with three membrane-spanning helices each (numbered I, II and III and IV, V and VI, respectively). According to an evolutionary model proposed by Hägerhäll and Hederstedt [9], the large single hydrophobic polypeptides of type B SQOR enzymes with five membrane-spanning helices are thought to have evolved from the fusion of the genes for the two small hydrophobic polypeptides with concomitant loss of transmembrane helix III. This view is supported by the structural superpositions discussed above (Section 3.2 and [11]). To a varying degree, all transmembrane segments are tilted with respect to the membrane normal [9,15].

The planes of both haem molecules bound by *W. succinogenes* QFR are approximately perpendicular to the membrane surface and their interplanar angle is 95°. The His axial ligands to the 'proximal' haem $b_P$, located towards the cytoplasmic surface of the membrane, and thus towards the [3Fe–4S] iron–sulphur cluster, are located on transmembrane helices II and V. Residues also of the two other transmembrane helices I and IV interact with the propionate groups of haem $b_P$ via hydrogen bonds and salt bridges, which underscores the structural importance of the bound haem [25]. The axial ligands to the 'distal' haem $b_D$ are located on helices I and IV. The binding of the two haem *b* molecules by an integral membrane protein four-helix bundle described here is very different from that described for other dihaem-binding membrane protein complexes, such as the cytochrome $bc_1$ complex [26], where only two transmembrane segments provide two axial haem *b* ligands each, and also the membrane-bound hydrogenases and formate dehydrogenases, where one transmembrane helix provides two axial His ligands and two others provide one His ligand each (see [27,28] for discussions). One consequence of this difference is that the distance between the two haem iron centres is distinctly shorter in *W. succinogenes* QFR (15.6 Å) than it is in the mitochondrial cytochrome $bc_1$ complex (21 Å) and in *E. coli* formate dehydrogenase-N (20.5 Å [29]). The mode of haem binding for the single (proximal) haem of *E. coli* SQR is analogous to that described for haem $b_P$ of *W. succinogenes* QFR.

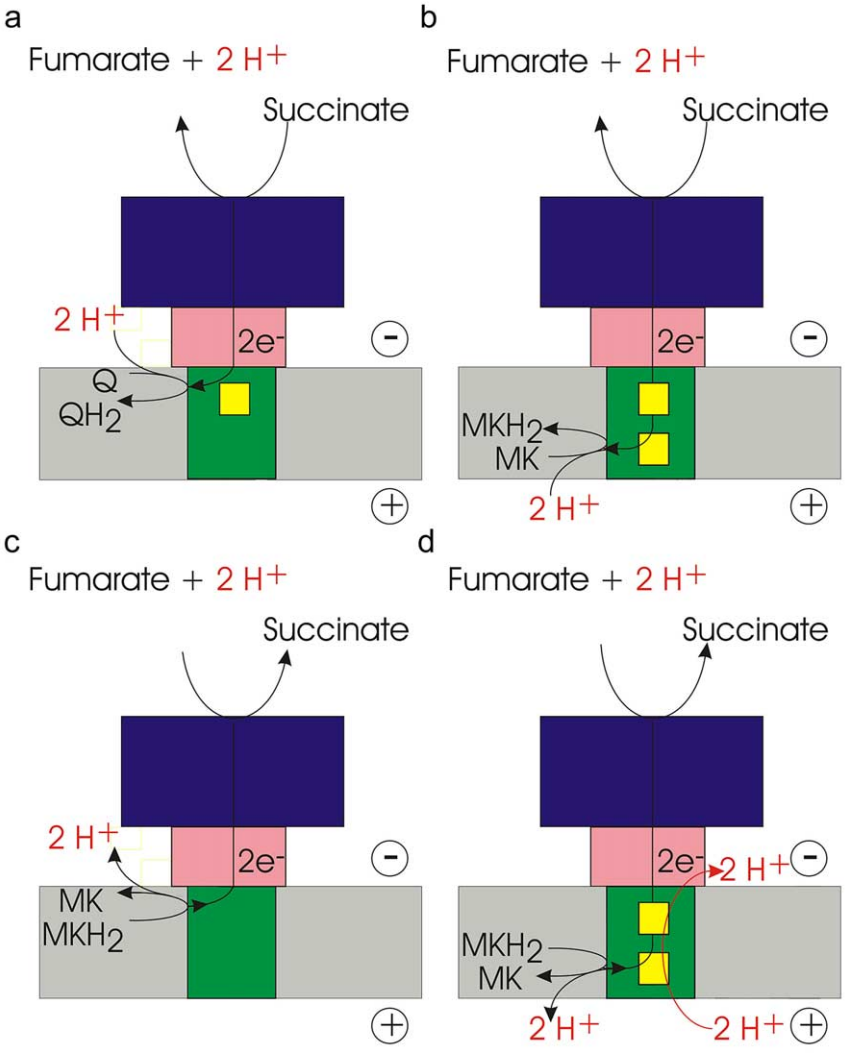


Fig. 4. The coupling of electron and proton flow in SQORs in aerobic (a,c) and anaerobic respiration (b,d). Positive and negative sides of the membrane are described for Fig. 1a. a,b: Electroneutral reactions as catalysed by C-type SQR enzymes (a) and D-type *E. coli* QFR (b). c: Utilisation of a transmembrane electrochemical potential $\Delta p$ as possibly catalysed by A-type and B-type enzymes. d: Electroneutral fumarate reduction by B-type QFR enzymes with a proposed compensatory 'E-pathway'.

The sites of quinol oxidation/quinone reduction have been localised in all three enzymes of known three-dimensional structure by a combination of X-ray crystallography, site-directed mutagenesis, functional characterisation of resulting variant enzymes and/or inhibitor-binding studies. In *E. coli* QFR, the menaquinol oxidation site is located 'proximally', close to the [3Fe–4S] cluster [30]. In *E. coli* SQR, this position is occupied by the haem *b* group, but the ubiquinone reduction site is also located proximally, close to the [3Fe–4S] cluster, at an alternative position [14]. In *W. succinogenes* QFR, the menaquinol oxidation site is located distally, close to haem $b_D$ [31].

## 4. Electron and proton transfer

### 4.1. Electron transfer

For the function of QFR, electrons have to be transferred from the quinol-oxidising site in the membrane to the fumarate-reducing site, protruding into the cytoplasm. Conversely, for the function of SQR, electrons have to be transferred from the succinate oxidation site in subunit A to the quinone reduction site in the membrane. The linear arrangement of the prosthetic groups in the complexes shown in Fig. 1b,c therefore provides one straightforward pathway by which electrons could be transferred efficiently between the two sites of catalysis. It has been shown for other electron transfer proteins that physiological electron transfer between prosthetic groups occurs if the edge-to-edge distances relevant for electron transfer are shorter than 14 Å, but not if they are longer than 14 Å [32]. In all three cases, this indicates that physiological electron transfer can occur between the prosthetic groups of one heterotrimeric or heterotetrameric complex, but not between the two (*W. succinogenes* QFR) or three (*E. coli* SQR) complexes in the respective homodimer or homotrimer.

Prior to the determination of the three-dimensional structures, because of its very low midpoint potential ($E_m < -250$ mV), the [4Fe–4S] iron–sulphur cluster had been suggested not to participate in electron transfer (see [3] for a discussion). However, the determined low potential may be an artifact due to anti-co-operative electrostatic interactions between the re-

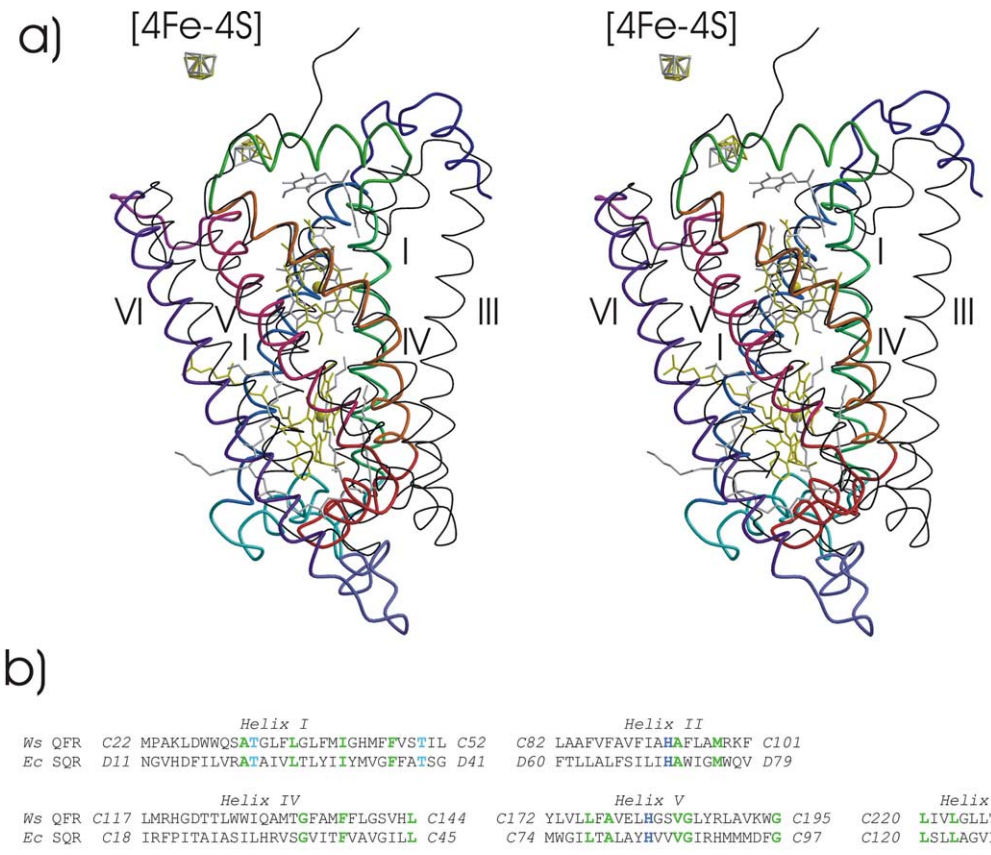


Fig. 5. a: Comparison of the transmembrane subunits from *W. succinogenes* QFR (in colour, with cofactors in yellow) and *E. coli* SQR (in black, with cofactors in grey). *W. succinogenes* QFR subunit C is coloured in dark blue (N-terminal helix), blue (transmembrane helix (TMH) I), light blue (periplasmic I–II helix), blue green (TMH II), green (cytoplasmic II–IV helix), orange (TMH IV), red (periplasmic IV–V helix), pink (TMH V), and purple (TMH VI). The [4Fe–4S] and [3Fe–4S] clusters are shown to aid orientation. b: Sequence comparison of the structurally aligned segments. Identical residues are emphasised.

dox centres [33]. The position of the [4Fe–4S] cluster as revealed in the structures is highly suggestive of its direct role in electron transfer between the [3Fe–4S] cluster and the [2Fe–2S] cluster. Despite this major thermodynamically unfavourable step, the calculated rate of electron transfer is on a microsecond scale, demonstrating that this barrier can easily be overcome by thermal activation as long as the electron transfer chain components are sufficiently close to promote intrinsically rapid electron tunneling [34].

The positioning of the haem in *E. coli* SQR is apparently puzzling, because it does not seem to be required for electron transfer between the catalytic sites. A possible explanation for this also explains why SQR is favoured over QFR in *E. coli* when oxygen is present. Under aerobic conditions, reduced *E. coli* QFR produces large amounts of reactive oxygen species (ROS), including superoxide radical ($O_2^-$) and hydrogen peroxide ($H_2O_2$), which has been suggested to be caused by electron accumulation around the FAD [35]. In sharp contrast, *E. coli* SQR reacts poorly with molecular oxygen, producing modest amounts of $O_2^-$ and no $H_2O_2$. On the basis of their crystal structure, Yankovskaya et al. [14] argue that the haem group in SQR provides an electron sink when the quinone site is not occupied, thus preventing buildup of electrons around the FAD and subsequent ROS generation. However, this electron sink mechanism is predicted to be less effective for mitochondrial SQRs because their haem *b* has a lower redox potential than that in *E. coli* SQR.

### 4.2. Electron-coupled proton transfer

In addition to the transfer of electrons, two protons are bound at the site of reduction and two protons are liberated at the site of oxidation (see reactions 1 and 2 and [36] for a review). An overview of the current status of discussion of electron and proton transfer in SQORs is shown in Fig. 4a–d. In mitochondrial complex II and other C-type enzymes, such as SQR from *P. denitrificans* and *E. coli*, electron transfer from succinate to ubiquinone does not lead to the generation of a transmembrane electrochemical potential $\Delta p$, since the protons released by succinate oxidation are on the same side of the membrane as those consumed by quinone reduction (Fig. 4a). Similarly, in *E. coli* QFR, the protons released by proximal quinol oxidation are balanced by the protons consumed by fumarate reduction (Fig. 4b). Succinate oxidation by menaquinone, an endergonic reaction under standard conditions, is catalysed by a B-type (Fig. 1a) SQOR in Gram-positive bacteria, e.g. *B. subtilis*. There is experimental evidence [37] indicating that the menaquinone reduction site in *B. subtilis* SQR is close to the haem $b_D$ in an analogous position to the menaquinol oxidation site of *W. succinogenes* QFR. This arrangement of the catalytic sites of succinate oxidation and menaquinone reduction would allow succinate oxidation by menaquinone in *B. subtilis* to be driven by the electrochemical proton potential (Fig. 4c) and there is indeed experimental evidence that this is the case [38]. This is the analogous reaction to that suggested by the arrangement of

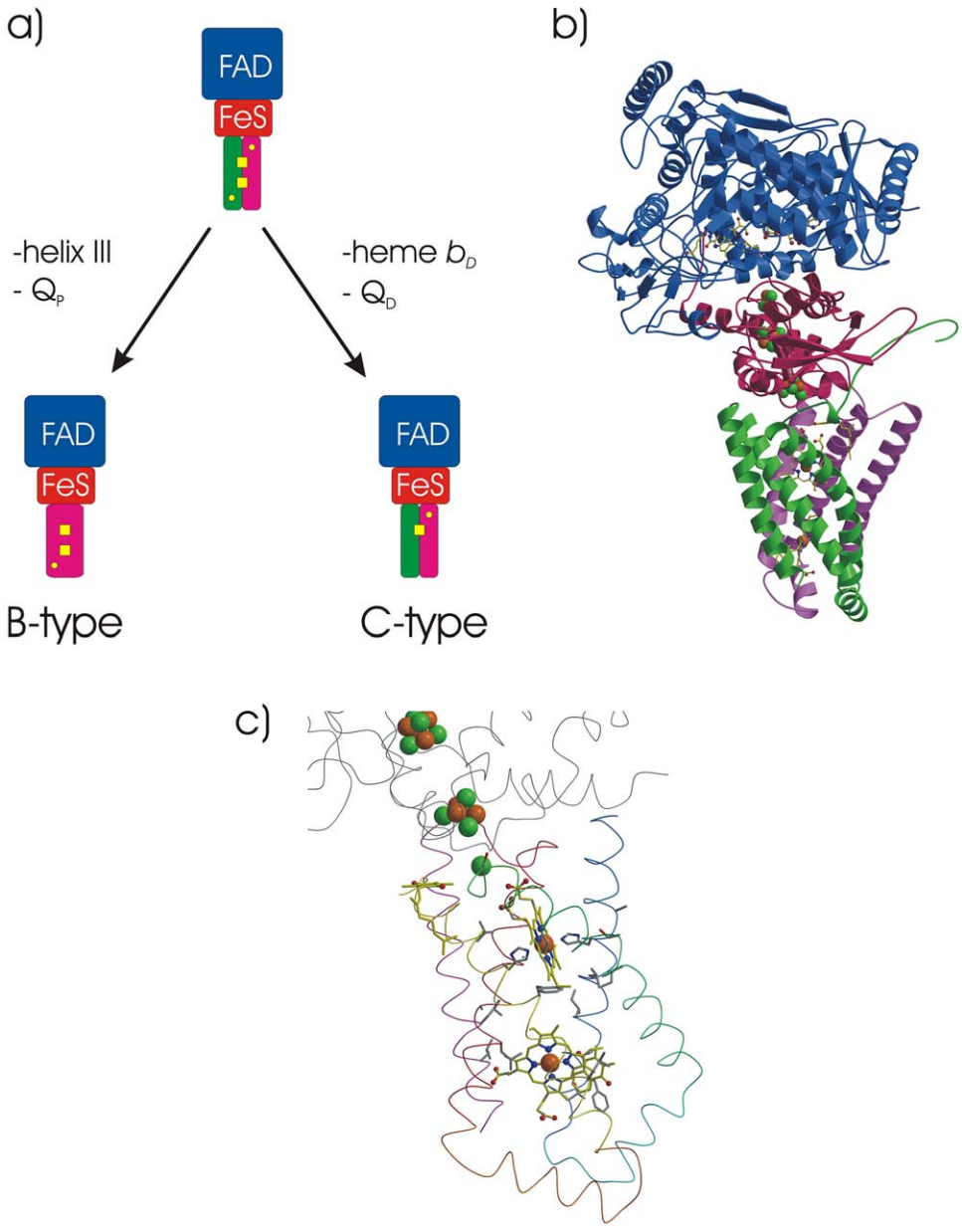


Fig. 6. Structural homology of *E. coli* SQR and *W. succinogenes* QFR suggests a common ancestor. a: Evolutionary scheme of the development of type B and type C SQOR enzymes from a hypothetical common ancestor (adapted from [10]). b: Hypothetical ancestral SQOR constructed from the co-ordinates of *W. succinogenes* QFR and *E. coli* SQR. Colour coding is analogous to Fig. 1. c: The transmembrane subunits of the hypothetical ancestor. Colour coding is analogous to Fig. 5a. The side chains of the residues found to be identical in Fig. 5b are shown.

the catalytic sites for *W. succinogenes* QFR, but in the opposite direction. Recent experimental results indeed indicate that *B. subtilis* SQR generates a proton potential when functioning as a QFR [39]. However, the experimental results on intact bacteria, with inverted vesicles or liposomes containing *W. succinogenes* QFR [40–42], indicate that the oxidation of menaquinol by fumarate as catalysed by *W. succinogenes* QFR is an electroneutral process. In order to reconcile these experimental findings with the arrangement of the catalytic sites in the structure, it has been proposed [27] that transmembrane electron transfer in dihaemic QFRs is tightly coupled to the compensatory, parallel transfer of protons across the membrane, thus balancing the protons released to the periplasm upon menaquinol oxidation and the protons bound from the cytoplasm upon fumarate reduction (Fig. 4d). A key residue in this proposed proton transfer pathway is a Glu residue located in the middle of the membrane that is conserved only in dihaemic menaquinol:fumarate reductases, but not in dihaemic succinate:menaquinone reductases [27]. First experimental results supporting this 'E-pathway hypothesis' have recently been obtained (Lancaster, Sauer, Groß, Haas, Mäntele, Simon and Madej, manuscript in preparation; Haas, Sauer, Groß, Simon, Mäntele and Lancaster, manuscript in preparation).

## 5. A model for an ancestral SQOR and the lack of evidence for a proximal quinone site in *W. succinogenes* QFR

The positions of 113 Cα atoms from *W. succinogenes* QFR and *E. coli* SQR could be superimposed with an rms deviation

of 1.8 Å, and Fig. 5a shows that most of this deviation can be accounted for by slight offsets of the secondary structure elements, indicating a very similar topology. The residues corresponding to the aligned Ca positions are shown in Fig. 5b. Of these 113 residues, 21 are identical, of which six are Leu, three Gly, three Ala, two His (the axial ligands to the proximal haem), two Thr, two Phe, one Ile, one Met, and one is a Val residue, and a number of other residues are similar.

It is generally thought that membrane-bound SQORs possess a common ancestor [10] with two hydrophobic polypeptides, two bound haems, and two quinone sites, $Q_D$ and $Q_P$. The structural similarities shown here support this idea, at least for B-type and C-type members of the superfamily (Fig. 6a). Thereby, B-type SQORs would have evolved from the common ancestor via loss of the proximal binding site $Q_P$ and fusion of the genes for the two small hydrophobic polypeptides with concomitant loss of transmembrane helix III. Conversely, C-type SQORs should have developed from the common ancestor by loss of the distal quinone $Q_D$ and haem $b_D$. A hypothetical model of such a common ancestor is shown in Fig. 6b,c.

It has been generally realised that the presence of a proximal quinone-binding site ($Q_P$) in addition to the distal quinone site ($Q_D$) and the two haem groups would allow the operation of a Q cycle mechanism in such an ancestral SQOR, analogous to that of the cytochrome $bc_1$ complex [43]. However, for *W. succinogenes* QFR, the available data indicate that such a scenario is not possible. Of the 10 residues found to form the $Q_P$ pocket of *E. coli* SQR [14], eight can be aligned in Fig. 5b and none of them are identical. The recent report by Pereira and Teixeira [44] of a $Q_P$-binding motif involving Leu C117, His C120, and Thr C123 in *W. succinogenes* QFR is apparently based entirely on a corresponding sequence motif of unknown accuracy. It is incompatible with the available crystal structure and with the published results from mutagenesis. In the structure, His C120 and Thr C123 are involved in the binding of subunit B, as has been described in detail earlier [45]. In addition, replacement of His C120 by Ala by site-directed mutagenesis indicates a non-essential role of this residue, since the resulting mutant is capable of growth with fumarate as the terminal electron acceptor [25]. The lack of any proof for the presence of a $Q_P$ site in *W. succinogenes* QFR favours a simpler mechanism of coupled electron and proton transfer, as represented by the E-pathway hypothesis, which adequately explains all available experimental data.

*Acknowledgements:* The author thanks his coauthors of the cited publications for their contributions. Support by DFG Sonderforschungsbereich 472 ('Molecular Bioenergetics', P19) is gratefully acknowledged.

## References

[1] Lancaster, C.R.D., Ed. (2002) Biochim. Biophys. Acta 1553, 1–176.
[2] Lemma, E., Hägerhäll, C., Geisler, V., Brandt, U., von Jagow, G. and Kröger, A. (1991) Biochim. Biophys. Acta 1059, 281–285.
[3] Hägerhäll, C. (1997) Biochim. Biophys. Acta 1320, 107–141.
[4] Saraste, M. (1999) Science 283, 1488–1493.
[5] Kröger, A. (1978) Biochim. Biophys. Acta 505, 129–145.
[6] Kröger, A., Geisler, V., Lemma, E., Theis, F. and Lenger, R. (1992) Arch. Microbiol. 158, 311–314.
[7] Lancaster, C.R.D. (2004) in: Respiration in Archaea and Bacteria, Vol. 1: Diversity of Prokaryotic Electron Transport Carriers (Zannoni, D., Ed.), Kluwer Scientific, Dordrecht, in press.
[8] Mitchell, P. (1979) Science 206, 1148–1159.
[9] Hägerhäll, C. and Hederstedt, L. (1996) FEBS Lett. 389, 25–31.
[10] Hederstedt, L. (1999) Science 284, 1941–1942.
[11] Lancaster, C.R.D., Kröger, A., Auer, M. and Michel, H. (1999) Nature 402, 377–385.
[12] Schäfer, G., Engelhard, M. and Müller, V. (1999) Microbiol. Mol. Biol. Rev. 63, 570–620.
[13] Iverson, T.M., Luna-Chavez, C., Cecchini, G. and Rees, D.C. (1999) Science 284, 1961–1966.
[14] Yankovskaya et al. (2003) Science 299, 700–704.
[15] Lancaster, C.R.D. and Kröger, A. (2000) Biochim. Biophys. Acta 1459, 422–431.
[16] Cecchini, G., Maklashina, E., Yankovskaya, V., Iverson, T.M. and Iwata, S. (2003) FEBS Lett. 545, 31–38.
[17] Singer, T.P. and McIntire, W.S. (1984) Methods Enzymol. 106, 369–378.
[18] Walker, W.H. and Singer, T.P. (1970) J. Biol. Chem. 245, 4224–4225.
[19] Kenny, W.C. and Kröger, A. (1977) FEBS Lett. 73, 239–243.
[20] Weiner, J.H. and Dickie, P. (1979) J. Biol. Chem. 254, 8590–8593.
[21] Lancaster, C.R.D., Groß, R. and Simon, J. (2001) Eur. J. Biochem. 268, 1820–1827.
[22] Gomes, C.M., Lemos, R.S., Teixeira, M., Kletzin, A., Huber, H., Stetter, K.O., Schäfer, G. and Anemüller, S. (1999) Biochim. Biophys. Acta 1411, 134–141.
[23] Manodori, A., Cecchini, G., Schröder, I., Gunsalus, R.P., Werth, M.T. and Johnson, M.K. (1992) Biochemistry 31, 2703–2712.
[24] Hägerhäll, C., Sled, V., Hederstedt, L. and Ohnishi, T. (1995) Biochim. Biophys. Acta 1229, 356–362.
[25] Simon, J., Groß, R., Ringel, M., Schmidt, E. and Kröger, A. (1998) Eur. J. Biochem. 251, 418–426.
[26] Xia, D., Yu, C.A., Kim, H., Xian, J.Z., Kachurin, A.M., Zhang, L., Yu, L. and Deisenhofer, J. (1997) Science 277, 60–66.
[27] Lancaster, C.R.D. (2002) Biochim. Biophys. Acta 1565, 215–231.
[28] Lancaster, C.R.D. (2003) Adv. Protein Chem. 63, 131–149.
[29] Jormakka, M., Törnroth, S., Byrne, B. and Iwata, S. (2002) Science 295, 1863–1868.
[30] Iverson, T.M., Luna-Chavez, C., Croal, L.R., Cecchini, G. and Rees, D.C. (2002) J. Biol. Chem. 277, 16124–16130.
[31] Lancaster, C.R.D., Groß, R., Haas, A., Ritter, M., Mäntele, W., Simon, J. and Kröger, A. (2000) Proc. Natl. Acad. Sci. USA 97, 13051–13056.
[32] Page, C.C., Moser, C.C., Chen, X. and Dutton, P.L. (1999) Nature 402, 47–52.
[33] Salerno, J.C. (1991) Biochem. Soc. Trans. 19, 599–605.
[34] Dutton, P.L., Chen, X., Page, C.C., Huang, S., Ohnishi, T. and Moser, C.C. (1998) in: Biological Electron Transfer Chains: Genetics, Composition and Mode of Operation (Canters, G.W. and Vijgenboom, E., Eds.), pp. 3–8, Kluwer Academic, Dordrecht.
[35] Messner, K.R. and Imlay, J.A. (2002) J. Biol. Chem. 277, 42563–42571.
[36] Ohnishi, T., Moser, C.C., Page, C.C., Dutton, P.L. and Yano, T. (2000) Structure 8, R23–R32.
[37] Matsson, M., Tolstoy, D., Aasa, R. and Hederstedt, L. (2000) Biochemistry 39, 8617–8624.
[38] Schirawski, J. and Unden, G. (1998) Eur. J. Biochem. 257, 210–215.
[39] Schnorpfeil, M., Janausch, I.G., Biel, S., Kröger, A. and Unden, G. (2001) Eur. J. Biochem. 268, 3069–3074.
[40] Geisler, V., Ullmann, R. and Kröger, A. (1994) Biochim. Biophys. Acta 1184, 219–226.
[41] Kröger, A., Biel, S., Simon, J., Groß, R., Unden, G. and Lancaster, C.R.D. (2002) Biochim. Biophys. Acta 1553, 23–38.
[42] Biel, S., Simon, J., Groß, R., Ruiz, T., Ruitenberg, M. and Kröger, A. (2002) Eur. J. Biochem. 269, 1974–1983.
[43] Mitchell, P. (1976) J. Theor. Biol. 62, 327–367.
[44] Pereira, M.M. and Teixeira, M. (2003) FEBS Lett. 543, 1–4.
[45] Lancaster, C.R.D. and Simon, J. (2002) Biochim. Biophys. Acta 1553, 84–101.
[46] Lancaster, C.R.D., in: Handbook of Metalloproteins, (Messerschmidt, A., Huber, R., Poulos, T. and Wieghardt, K., Eds.), pp. 379–401, John Wiley and Sons, Chichester.
[47] Kraulis, P.J. (1991) J. Appl. Crystallogr. 24, 946–950.
[48] Esnouf, R.M. (1997) J. Mol. Graphics Mod. 15, 132–134.
[49] Merrit, E.A. and Bacon, D.J. (1997) Methods Enzymol. 277, 505–524.